Carbonmonoxy Horseradish Peroxidase as a Function of pH and Substrate: Influence of Local Electric Fields on the Optical and Infrared Spectra†

A. D. Kaposi,‡ W. W. Wright,§ J. Fidy,‡ S. S. Stavrov,|| J. M. Vanderkooi,*,§ and I. Rasnik§

Department of Biophysics and Radiation Biology, Semmelweis University Faculty of Medicine, Puskin u. 9, Budapest H-1088, Hungary, Johnson Research Foundation, Department of Biochemistry and Biophysics, University of Pennsylvania School of Medicine, Philadelphia, Pennsylvania 19104-6059, and Department of Human Genetics and Molecular Medicine, Sackler Institute of Molecular Medicine, Sackler School of Medicine, Tel Aviv University, Ramat Aviv, P.O. Box 3904, Tel Aviv 69978, Israel

Received December 7, 2000; Revised Manuscript Received January 16, 2001

ABSTRACT: Infrared and optical spectra of carbonmonoxy horseradish peroxidase were monitored as a function of pH and substrate binding. The analyses of experimental results together with semiempirical calculations show that the CO−porphyrin complex is sensitive to environmental changes. The electronic Q(0,0) band of the porphyrin and the CO stretching mode respond to external perturbations with different symmetry dependencies. In this way, the complex is nonisotropic, and the combined spectral analyses constitute a valuable tool for the investigation of structure. In the absence of substrate and at pH 6.0, the low-spin heme optical Q(0,0) absorption band is a single peak that narrows as the temperature decreases. Under these conditions, the CO vibrational stretch frequency is at 1903 cm^{-1}. Addition of the substrates benzohydroxamic acid or naphthohydroxamic acid produces a split of ∼320 cm^{-1} in the Q(0,0) absorption band that is clearly evident at <100 K and shifts the CO absorption to 1916 cm^{-1}. Increasing the pH to 9.3 also causes a split in the Q(0,0) optical band and elicits a shift in ν(CO) to a higher frequency (1936 cm^{-1}). The splitting of the Q(0,0) band and the shifts in the IR spectra are both consistent with changes in the local electric field produced by the proximity of the electronegative carbonyl of the substrate near the heme or the protonation and/or deprotonation of the distal histidine, although other effects are also considered. The larger effect on the Q(0,0) band with substrate at low pH and the shift of ν(CO) at high pH can be rationalized by the directionality of the field and the orientation dependence of dipolar interactions.

A question for all enzymes is how the polypeptide chain modulates the activity of a prosthetic group in a specific manner. For heme proteins, this question is especially intriguing in view of these proteins' diverse functions, including transport of O_2, electrons, and protons, enzymatic reactions, including hydroxylation, oxygenation, and oxidative phosphorylation, and also cellular regulation. The prosthetic group for enzymes carrying out these roles is rather simple, a heme. The reactions, for the most part, occur at the Fe core, but to understand the specificity of the reactivity of Fe, one must think of the whole porphyrin−metal−ligand complex and its modification by the polypeptide chain.

The peroxidases, one subgroup of heme proteins, react with H_2O_2 to form H_2O. A well-studied member of this family is horseradish peroxidase (HRP).[1] H_2O_2 serves as the oxidant in most of its reactions, but in contrast, a wide variety of aromatic substrates (AH) of HRP can serve as H-donor reductants. The enzymatic scheme for the catalysis carried out by HRP is given in Scheme 1. Adding H_2O_2 to the resting enzyme produces compound I (*1*). The resting enzyme also can bind the aromatic substrate, AH, concomitant with a characteristic absorption change in the heme spectra (*2*−*4*). The random nature of substrate binding allows the independent study of compound I, Fe^{3+}HRP, and Fe^{3+}HRP-AH. The structure of Fe^{3+}HRP is known (*5*), and structures are also available for Fe^{3+}HRP-AH, where AH is benzohydroxamic acid (BHA) (*6*) or ferulic acid (*7*). The X-ray structure shows that BHA is located near the heme, but not directly bonded

Scheme 1

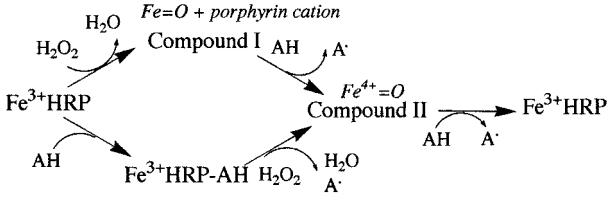

† This work was supported by the National Institutes of Health (Grants RO1 GM 55004 and PO1 GM48130), the National Science Foundation (Grant NT 98123221), the Hungarian Academy of Science (122/1998), Hungarian Grants FKFP 1191/1997 and OTKA25545, and Israeli Grant CaMeO.

* To whom correspondence should be addressed. E-mail: vanderko@mail.med.upenn.edu. Phone: (215) 898-8783. Fax: (215) 573-2042.

‡ Semmelweis University Faculty of Medicine.

§ University of Pennsylvania School of Medicine.

|| Tel Aviv University.

[1] Abbreviations: HRP, horseradish peroxidase type C; NHA, naphthohydroxamic acid; BHA, benzohydroxamic acid; FDPB, finite-difference Poisson−Boltzmann; ZINDO, Zerner intermediate neglect of differential overlap.

10.1021/bi002784z CCC: $20.00 © 2001 American Chemical Society
Published on Web 03/01/2001

Scheme 2

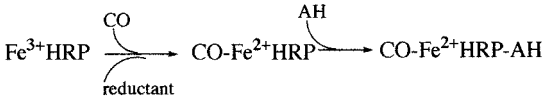

to Fe, a conclusion in accord with earlier NMR studies (*2*, *8*, *9*) and computer modeling (*10*).

HRP can exist in various low-spin forms. Compound II can be converted into an inactive ferrous low-spin O_2 complex, called compound III. An analogous low-spin complex is formed when the resting enzyme is reduced in the presence of CO (Scheme 2) (*11*). The CO complex can bind the aromatic substrate to form a stable low-spin tertiary complex. The absorption spectra of low-spin metal porphyrin complexes are quite well understood. They have a distinguishing intense transition in the region of 400−430 nm (23000−25000 cm^{-1}), called the Soret or B band and a weaker transition, Q(0,0) or α band, with an associated vibronic band, Qv or β band, in the visible region at 530−590 nm (17000−19000 cm^{-1}). Work by Gouterman and others has led to the assignment of these transitions to excitations from a_{1u}, a_{2u} porphyrin π to e* g porphyrin π* orbitals, forming four one-electron excited states which mix by configuration interaction (*12*). Porphyrin electronic transitions in heme proteins are sensitive to the protein environment due to a high susceptibility of the π electron cloud to perturbations by the surrounding protein.

HRP is an especially intriguing protein for studying how the heme is affected by perturbations, because its spectra can be changed by binding substrate or by changing pH, as indicated above. The Q(0,0) absorption band of Mg mesoporphyrin which was used to replace the heme of HRP (resulting in a low-spin metal-bound porphyrin) shows a composite nature in the presence of the substrate NHA at low temperatures, and with hole burning studies, the spectral features can be ascertained as spectral splitting (*13*, *14*). The general sensitivity of heme optical spectra to the protein matrix is indicated by a frequently observed split in the Q(0,0) absorption band of low-spin ferrous hemes (*15*, and references therein). Using computational methods, it was concluded that the splitting can be ascribed to protein internal electric fields, as well as protein-induced distortion of the ring (*16*, *17*) and additional effects from ligation and ring substitution (*18*). Whether the sensitivity to the protein environment of the Q(0,0) band is a general feature for other low-spin forms of the protein, including CO-HRP, has not been determined. In addition to its optical spectrum, the carbonmonoxy form of the enzyme is of interest because it can also be studied through the IR signal of the bound CO. Experimental differences in CO stretch frequency are observed in homologous proteins and single-mutant derivatives of proteins (*19*−*24*), consistent with the interpretation that the CO frequency is extremely sensitive to the conformation of the heme and local electric fields (*25*−*31*).

Because of the complexity of the heme pocket in these proteins, changes in experimental conditions can affect the CO IR frequency and the optical spectra through many factors. The analyses of both electronic and IR spectra reduce the number of variables to be considered, since only the environmental changes consistent with both spectra should be considered. In first-order perturbation theory, the spectral shifts of the CO stretch frequency can be considered proportional to the interaction energy of the CO dipole with the electrostatic potential produced by the environment. As shown below, this interaction is proportional to the scalar product of the CO dipole moment with the external electrostatic field, defining a preferential axis (in the direction of the CO dipole moment). On the other hand, the porphyrin Q(0,0) electronic band splitting is produced by a break of the D_{4h} symmetry, so the macrocycle plane is the reference for the analyses of these perturbations.

In this paper, we inspect the electronic spectra of the heme and the IR signal of CO bound to HRP as a function of pH and the binding of the aromatic substrates BHA and naphthohydroxamic acid (NHA). We show that when the substrate is added or when pH is increased the Q(0,0) band of CO-HRP splits and the CO vibrational frequency shifts. Changes in both spectral markers are consistent with pH and substrate-induced changes in the local fields near the heme.

MATERIALS AND METHODS

Water was deionized and then glass distilled. Type C HRP was obtained from Sigma Chemical Co. (St. Louis, MO). Aldrich Chemical Co. (Milwaukee, WI) supplied BHA, and NHA was purchased from ICN (Costa Mesa, CA). HRP was purified as described previously (*32*) based upon the procedure of Paul (*33*). The CO derivative of HRP was prepared as follows. Seventy microliters of a 60/40 (v/v) glycerol/water solution was placed in a 25 mL round-bottom boiling vessel that was fitted with a side valve to introduce a vacuum and CO and a sidearm to hold dry components. Seven milligrams of HRP and 1 mg of sodium dithionite were placed in the sidearm. The assembly was aspirated for 15 min to remove air. CO was introduced into the vessel for ∼15 min at 8−10 psi, and then the vessel was closed. The dry components from the sidearm were then introduced to the solution and mixed by swirling. The solution became bright orange/red. The solution was allowed to remain in the CO atmosphere for 0.5 h, at which time the vessel was opened. The pH values were adjusted by adding HCl or NaOH. The final pH values, 6.0 and 9.3, are given in the figure legends. The final protein concentration was in the 2−4 mM range.

IR spectra were obtained with a Bruker IFS 66 Fourier transform IR instrument (Bruker, Brookline, MA) that was configured with a Globar source, a KBr beam splitter, and a liquid nitrogen-cooled MCT detector (*34*). A transmission cell holder with CaF_2 windows was used to hold the sample. The spacer width was 200 μm. Spectra were an average of 128 interferograms recorded at a resolution of 2 cm^{-1}. A four-point apodization function and a zero-filling factor of 2 were used with the Opus acquisition software. The acquisition time for each spectrum was ∼2 min. The baseline was corrected by straight line correction when the peaks were fit to a Gaussian function using PeakFit (Jandel Scientific, San Rafael, CA). A Hitachi Perkin-Elmer absorption instrument was used to record the UV−visible absorption spectra. The same transmission cell holder used for the IR measurements was used to hold the sample, but the spacer width was 100 μm for the optical measurements. The thin spacer and the use of the cryogenic cosolvent glycerol ensured that the sample remained optically clear with no cracks over the entire temperature range. The temperature was regulated

using an OmniPlex cryostat (APD Cryogenics, Allentown, PA). The spectra at high temperatures were obtained first; the temperature was reduced by 10 °C, and then the next spectrum was obtained. The equilibration time at each temperature was ~10 min. In certain experiments, absorption spectra were again taken as the temperature increased. No irreversible effects were seen.

Electrostatic Calculations. As the crystallographic structure of CO-bound horseradish peroxidase is not known, we used for our calculations the HRP structure in the presence of benzohydroxamic acid substrate as given in the Protein Data Bank entry 2ATJ. The CO was added to the structure file with standard bond lengths and a bent orientation with the Biopolymer module of the InsightII package (Biosym Technologies, San Diego, CA) as described by Laberge et al. (*21*). Because of the calculation method used in this work, this approximate structure is accurate enough for our purpose. It should be noted that this structure was used for all three calculations so that the calculated differences are due solely to the imposed electric potential, and not differences in starting structures.

The electrostatic potential produced by the CO dipole was calculated with the finite-difference Poisson−Boltzmann (FDPB) method as implemented in the Delphi package (*35*−*38*). The protein solvent system was modeled as a two dielectric system with the boundary defined by the protein molecular surface, with dielectric constants of 80 for water and 2 for the protein. A 65 × 65 × 65 grid was used, and the scale was chosen so the longest protein dimension was 70% of the grid length. The ionic strength of the solvent was taken to be 0.01 M. More details of this method can be found elsewhere (*21*, *26*, *39*).

The benzohydroxamic acid structure was minimized in energy, and the partial charges were calculated at a Hartree−Fock level using the Gaussian 94 program (Gaussian, Pittsburgh, PA) (*40*). The main contributions (in units of *e*, with hydrogens atomic charges summed into heavy atoms) are from the hydroxamic functional group, 0.70 *e* for C, −0.59 *e* for O1 (bound to C), −0.10 *e* for N, and −0.08 *e* for O2 (bound to N).

Estimation of the CO Stretch Vibrational Frequency. As the protein environment is difficult to model exactly, calculation of the absolute values of the vibrational frequency will present limited accuracy. On the other hand, vibrational frequency shifts are more easily calculated and reliable. In this work, we calculate the CO stretch frequency shift, following the procedure of Laberge et al., which combines the FDPB method and the use of an empirical Stark tuning rate to evaluate electrostatically induced shifts in CO stretch frequency (*21*, *26*). The empirical values obtained by Lambert (*41*) to calculate vibrational frequency shifts due to the vibrational Stark effect have proven to give good agreement with experimental results for a series of proteins (*21*).

The method of calculation makes use of the concept of the empirical Stark tuning rate, defined as

$$\delta\nu = \mathrm{d}\nu_{01}/\mathrm{d}E \tag{1}$$

where ν_{01} is the energy difference between the $\nu = 0$ and $\nu = 1$ states and E the electrostatic field module of the component in the CO dipole direction. The experimental and calculated values of $\delta\nu$ are in excellent agreement, as in previous works we use a value of 4.9×10^{-7} cm^{-1}/(V^{-1} cm^{-1}). In the dipole approximation, the perturbation of the vibrational energy levels is given by the interaction of the dipole moment of CO with the electric field. The frequency shift due to an external electric field $\vec{E}$ will be given by

$$\Delta\nu = \delta\nu\left(\frac{\hat{\mu}_{\mathrm{CO}}\vec{E}}{|\hat{\mu}_{\mathrm{CO}}|}\right) \tag{2}$$

where $\hat{\mu}_{\mathrm{CO}}$ is the dipole vector along the C−O bond. Because the interaction energy (term within parentheses) of a dipole with the electric field produced by a set of charges must be equal to the interaction energy of these charges with the field produced by the dipole, eq 2 can be rewritten as

$$\Delta\nu = \frac{\delta\nu}{|\hat{\mu}_{\mathrm{CO}}|}\sum_i q_i\Phi_i(\hat{\mu}_{\mathrm{CO}}) \tag{3}$$

where q_i is the i point charge and $\Phi_i(\hat{\mu}_{\mathrm{CO}})$ is the potential produced by the dipole at the charge site. This form is far more convenient for our calculations. The field of the dipole is calculated for the protein−solvent system within a FDPB approach, and the contribution to the shift of each charged residue of interest may be calculated independently. Once the potential map was obtained for the system, the spectral shift of the CO stretch band was calculated to be $1.22 q_i\Phi_i$ cm^{-1} (the potential in units of kT per electric charge, as obtained from the Delphi calculations) summed over the charges of the residue or molecule (substrate) of interest. The factor 1.22 accounts for the unit's conversion factor, the Stark tuning rate, and the dipole moment of CO.

Estimation of Optical Spectral Features. Quantum chemical calculations of the optical spectra used the intermediate neglect of differential overlap (INDO/s) semiempirical method that was parametrized for porphyrin spectroscopy by Zerner and co-workers (*42*−*44*). In as much that the coordinates are not known, we simulated spectral features in the same way as reported previously (*16*), with the CO geometry discussed in the electrostatic calculations section. The results of the calculations for the Q-band splitting are sensitive to the particular macrocycle conformation and CO geometry. We used this method as an indication that the observed experimental splittings are compatible with the variations in electrostatic potential at the macrocycle for the different conditions analyzed in this work. As was done previously (*18*), 59 configurations, the maximum allowed by the program, were used. The Q and B transition can be very well described with this number of configurations as they involve few excited states. We tested the dependence of our results using fewer configurations with the same results, indicating that the number of configurations used to evaluate these low-energy-lying transitions gives reliable results.

In previous work (*16*−*18*), it was shown that the spectral splitting of the heme group in proteins is caused by a combined effect of symmetry-lowering factors. When a certain protein family or a protein under different experimental conditions is compared, it is extremely useful to have quantitative methods of comparing the different environments and conformations. For example, the macrocycle conforma-

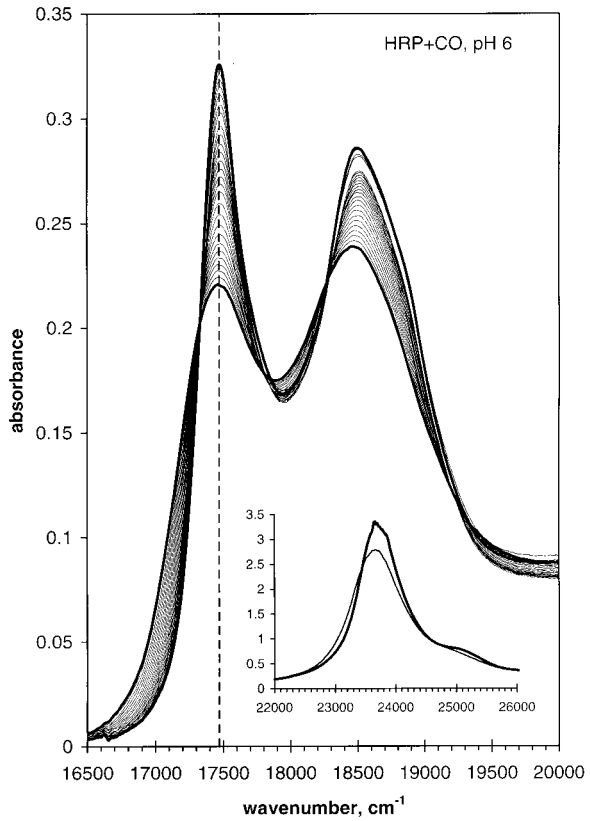

FIGURE 1: Optical absorption of CO-HRP at pH 6.0. The sample contained a 60% (v/v) glycerol/water mixture and 10 mM sodium phosphate buffer. The dashed line at 17 470 cm^{-1} marks the Q(0,0) band position. The dark line at lower absorbance at this frequency is the spectrum at 290 K, and the upper dark line is the spectrum at 11−13 K. The sample was stepwise cooled by 10 °C, and spectra were taken every 10 °C. These spectra are shown with light lines, as a series with the increasing absorbance at 17 470 cm^{-1} occurring with a decrease in temperature. The inset shows the Soret region absorbance: dark line, 11−13 K; and light line, 290 K.

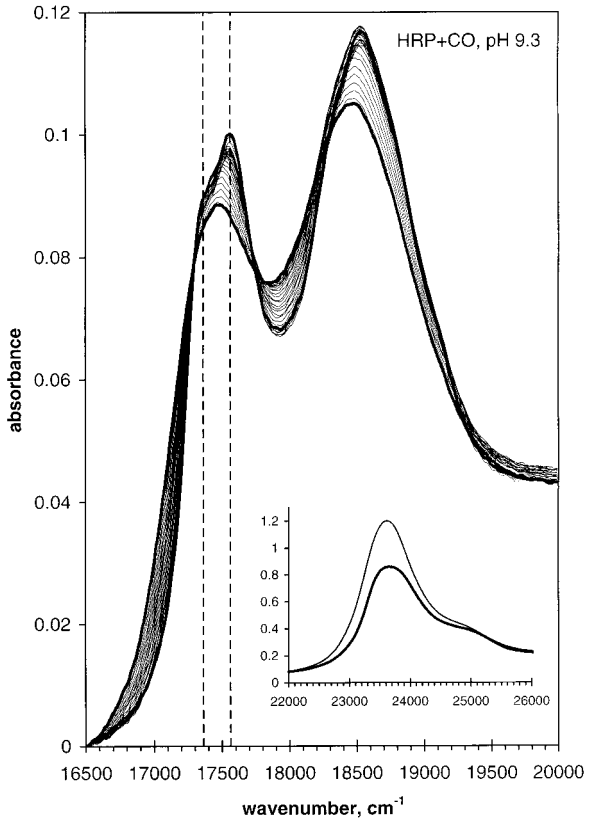

FIGURE 2: Optical absorption of CO-HRP at pH 9.3. Other conditions are the same as described in the legend of Figure 1. Dashed lines at 17 362 and 17 562 cm^{-1} mark the split Q(0,0) band peaks. The dark line at lower absorbance at these frequencies is the spectrum taken at 290 K, and the higher absorbance spectrum was at 12 K. Lighter lines are spectra taken as described in the legend of Figure 1. The inset shows the Soret region absorbance: dark line, 12 K; and light line, 290 K.

tional analysis of Jentzen et al. (*45*−*48*) allows the comparison of heme macrocycle conformations in a quantitative way, in terms of a normal mode decomposition. In a similar way, we developed a program that can be used to decompose the electrostatic potential in a spatial region in terms of the irreducible representations of a particular point group. The electrostatic potential, as obtained for example from a FDPB calculation, can be expressed as a sum of contributions, each belonging to a particular irreducible representation of the point group (*48*). In particular, for heme groups in proteins, the electrostatic potential exerted by the rest of the protein at the heme site can be decomposed into the 10 irreducible representations of the D_{4h} group. A discussion of the influence of the symmetry of external perturbations to mix the Q_x, Q_y, B_x, and B_y states has been given in detail, for example, in the paper of Gouterman (*49*). This method allows the automatic elimination from the electrostatic potential of the components that introduce no changes in the spectra based on group theory considerations. In the D_{4h} group, the symmetric product $[E^*E] = A_{1g} + B_{1g} + B_{2g}$, and therefore, only these components can contribute to the spectral features of the Q-band. For distorted porphyrin rings, the selection rules valid for a planar macrocycle may be relieved, as the distortion may change the symmetry of the molecular orbitals (*16*). Because the X-ray structure is not available for the protein complexes discussed in this work, we calculated the electrostatic potential at the heme site for the same CO structure used for the other calculations.

RESULTS

Visible Absorption Spectra. Kaposi et al. have determined that HRP in a glycerol/water matrix remains folded in the temperature range of 300−13 K as indicated by the IR spectrum of the amide I′ and II′ bands (*32*). Visible absorption spectra of the CO−HRP complex, given in Figure 1 at temperatures ranging from ambient to ∼10 K, show two bands in visible region (at 541 nm, 18 480 cm^{-1}, and 572 nm, 17 480 cm^{-1}), typical of low-spin hypsoporphyrins (*50*). The Soret band maximum is at 423 nm, 23 640 cm^{-1}. The peak positions are the same as reported previously for this compound at room temperature (*51*). As the temperature is lowered, the Q(0,0) band becomes narrower, and the absorption at the peak maximum increases. The Q(0,0) band is centered at 572.5 nm, 17 467 cm^{-1}, at 20 K.

At alkaline pH values, HRP undergoes spectroscopic changes and the residue responsible for the change has a p*K* of ∼8.3 (*52*, *53*). On the basis of the pH dependence of site-mutated enzymes, this residue is identified as His42, which has its p*K* modulated by interaction with Arg38 (*23*, *54*). The absorption spectrum of CO-HRP at high pH is documented in Figure 2. At room temperature, the Q(0,0) band broadens relative to that of the low-pH form (compare with Figure 1), and the band no longer appears symmetrical. At

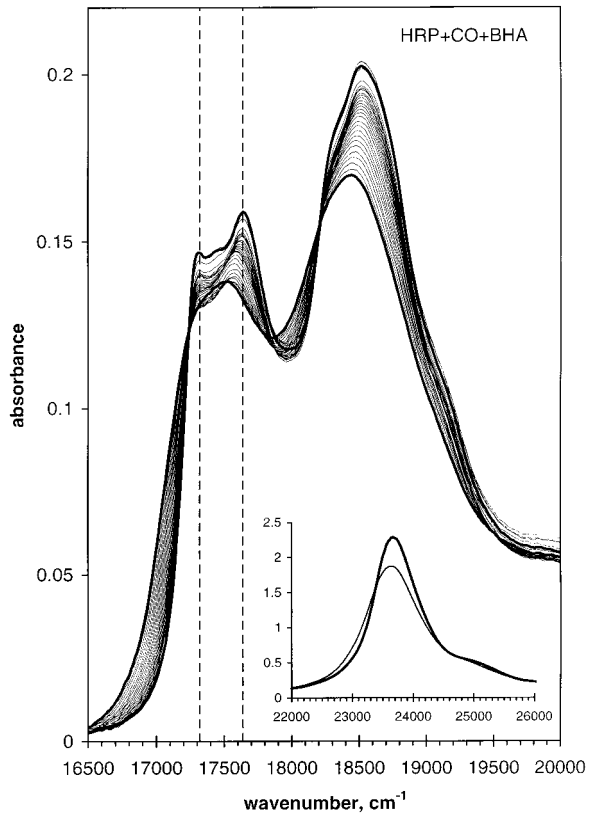

FIGURE 3: Optical absorption of the CO-HRP−BHA complex at pH 6.0. The BHA concentration was ∼3 mM. Other conditions are the same as described in the legend of Figure 1. Dashed lines at 17 320 and 17 640 cm^{-1} mark the split Q(0,0) band peaks. The dark line at lower absorbance at these frequencies is the spectrum taken at 290 K, and the dark line at higher absorbance is the spectrum taken at 13 K. Lighter lines are spectra taken as described in the legend of Figure 1. The inset shows the Soret region absorbance: dark line, 13 K; and light line, 290 K.

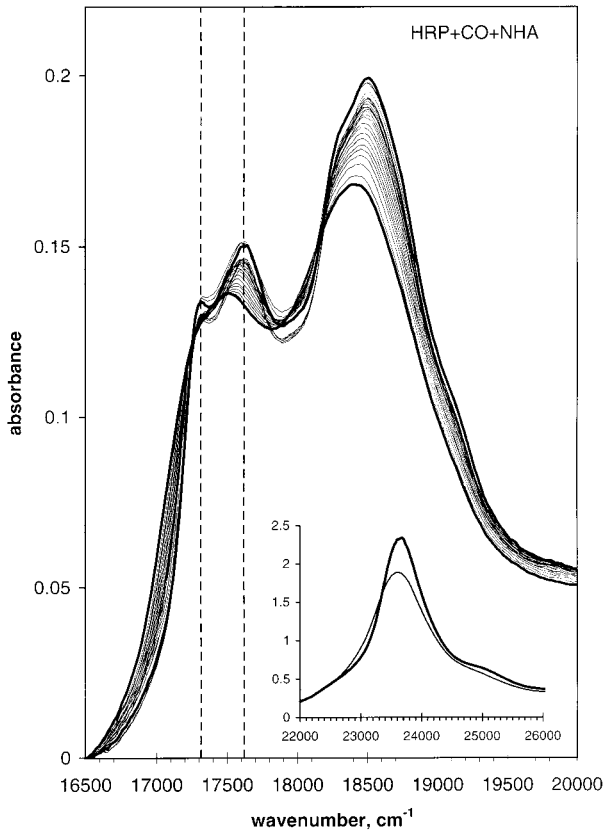

FIGURE 4: Optical absorption of the CO-HRP−NHA complex at pH 6.0. The NHA concentration was ∼3 mM. Other conditions are the same as described in the legend of Figure 1. Dashed lines at 17 313 and 17 618 cm^{-1} mark the split Q(0,0) band peaks. The dark line at lower absorbance at these frequencies is the spectrum taken at 290 K, and the dark line at higher absorbance is the spectrum taken at 13 K. Lighter lines are spectra taken as described in the legend of Figure 1. The inset shows the Soret region absorbance: dark line, 13 K; and light line, 290 K.

the lowest temperatures where the spectral resolution is the highest, it is evident that the Q(0,0) band is split.

Addition of the BHA substrate to the enzyme also significantly affects the spectra under consideration. The electronic spectrum for CO-HRP in the presence of BHA at pH 6.0 is shown in Figure 3. As in the case for high pH values, even at room temperature it is apparent that the Q(0,0) band is broadened relative to that of the substrate-free enzyme (cf. Figure 1), and as the temperature decreases, the split in the band is plainly visible. The lower peak is at 567 nm, 17 640 cm^{-1}, and the upper peak is at 578 nm, 17 320 cm^{-1}. The split is ∼320 cm^{-1}. The mean position is at 17 469 cm^{-1}, the same as the maximum seen for substrate-free CO-HRP within experimental error (Figure 1). In other words, the binding of substrate to CO-HRP does not appreciably shift the spectrum but only splits the band.

Like BHA, the substrate analogue NHA binds to HRP with high affinity (*3*). As seen in Figure 4, the optical spectra are similar to those observed for the BHA complex (Figure 3). The frequency of the split, ∼305 cm^{-1}, is close to that observed for the BHA complex.

The values for the splitting of the Q(0,0) band for the CO-HRP are summarized in Table 1, which also gives the Q(0,0) band splitting for HRP in which the heme was substituted with Mg-mesoporphyrin (Mg-MP-HRP) (*55*).

Infrared Absorption Spectra. The IR spectrum of CO bound to the enzyme was examined for the samples under the same conditions used for the optical studies. In the purified enzyme used in our study, a single absorption band at 1903 cm^{-1} was seen for CO-HRP and at 1937 cm^{-1} for pH 9.3; this is shown in Figure 5A. [Other workers have reported that there are two CO absorption bands in the IR spectra of carbonmonoxy HRP (*56*−*58*). The pH is known to affect the ratio of the two peaks (*58*), and therefore, the medium conditions may perhaps account for the difference between our results and the literature.] Figure 5A also shows the IR absorption band of CO-HRP in the presence of BHA. In this sample, the major absorption band is at 1916 cm^{-1}. It is evident in Figure 5 that there is some protein that does not have substrate bound, since the peak observed at 1903 cm^{-1} is at the same frequency as for the substrate-free protein. Assuming that the CO vibrational mode extinction

Table 1: Splitting in the Q(0,0) Band of Low-Spin Forms of HRP[a]

	split (cm^{-1})	ref
CO-HRP	not detected	this work
CO-HRP, pH 9.3	200	this work
CO-HRP with BHA	320	this work
CO-HRP with NHA	305	this work
Mg-MP-HRP	96	*55*
Mg-MP-HRP with NHA	254	*55*

[a] pH 6.0 except where indicated. The temperature of measurement in this work was 20 K.

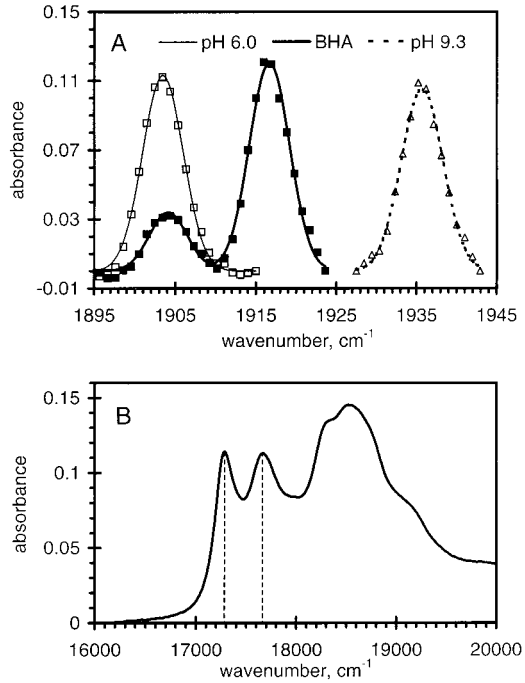

FIGURE 5: (A) Infrared absorption of CO-HRP, the CO-HRP−BHA complex at pH 6.0, and CO-HRP at pH 9.3. The symbols represent data points after linear baseline subtraction. Connecting lines are fitted Gaussians functions. (B) Optical spectra of the CO-HRP−BHA spectra at pH 6.0 minus a contribution from CO-HRP. The temperature was 20 K.

Table 2: CO Frequencies[a]

	temperature (K)	frequency (cm^{-1})	ref
HRP	293	1903	this work
	293	1904	*57*, *65*
	20	1903	this work
HRP, pH 9.3	293	1936	this work
	293	1932	*52*
	20	1936	this work
HRP with BHA	293	1911	this work, *52*
	20	1916	this work
HRP with NHA	293	1916	this work
	20	1916 (1919)	this work

[a] pH 6.0 except where indicated.

constant is about the same for the substrate-bound and -free forms, we can estimate that ~80% of the protein has BHA bound. To make sure that the perceived splitting of the Q(0,0) band was not due to the free form, the spectrum of the free form was subtracted from that of the BHA-bound protein (Figure 5B). The difference spectrum clearly shows the spectral splitting in this band.

In the complexes of HRP-CO with NHA, the CO stretch frequency in the presence of this substrate was at 1916 cm^{-1} with a second smaller peak at 1919 cm^{-1} apparent at low temperatures (not shown). Therefore, in the optical spectrum (Figure 4), there will also be some contribution from this second form of the enzyme. Nevertheless, a clear spectral splitting was seen.

The frequencies of the CO stretch are given in Table 2.

Evaluation of Infrared Spectral Shifts. We took for the charged group of the substrates the same spatial coordinates (available for BHA acid in the Protein Data Bank file), so the calculated shift in ν(CO) obtained by binding either BHA and NHA is the same. In the structure, the electronegative

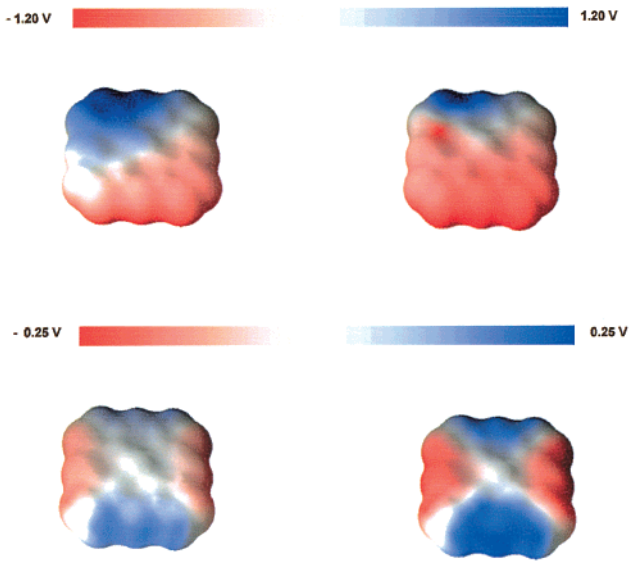

FIGURE 6: Electrostatic potential calculated at the heme site. The cycle is viewed from the CO side, and the propionic acids are toward the top: (top) the total electrostatic potential, (bottom) the B_{1g} component of the electrostatic potential, (left) low pH, and (right) low pH with substrate.

O of the BHA carbonyl group is oriented toward the CO bound to the heme. BHA is a weak acid with an aqueous pK_a of 8.8; when BHA is bound to the enzyme, the pK would likely be even higher. If it is assumed that the acids are protonated (and therefore formally uncharged) at pH 6.0, the calculated spectral shift obtained for the field change produced by the presence of the substrate is 6 cm^{-1}.

For the distal histidine residue, we considered a change of −1 in the charge of the NE2 nitrogen on going from pH 6.0 to 9.3. In this case, the calculated spectral shift in ν(CO) is 27 cm^{-1}.

These results are in good agreement in both sign and magnitude with the experimental ones (see Table 2).

Evaluation of the Optical Band Split. We performed ZINDO quantum chemical calculations [as described previously (*18*)]. The calculated splitting for the distorted CO−heme complex in the absence of a field was 60 cm^{-1}. Using the field for the protein−CO complex at low pH gave a calculated splitting of 80 cm^{-1}. For the protein−CO complex at high pH, this value was 150 cm^{-1}, and it became 280 cm^{-1} for the protein−CO-BHA complex. These calculated values are in good agreement with the trend seen in the experimental results. As noted above, the starting structures used for the calculations are the same, so these splittings represent the effect of the electric field only.

In the top panel of Figure 6, we show the total calculated electrostatic potential at the heme molecular surface for the experimental case of low pH and with the addition of BHA. Although the results for these cases exhibit differences, suggesting that the change in experimental conditions introduces an effective change in the electrostatic potential at the heme group, it is not clear from these figures how the potential should affect the transition. In the lower part of the figure, we show the component of the electrostatic potential belonging to the irreducible representation b_{1g} of the D_{4h} group. In this case, it is very clear that the addition of the substrate introduces a major difference in this symmetry component of the total electrostatic potential

(Figure 6, bottom right). The correlation between spectral splitting and the change in this component of the electrostatic potential is evident. A similar comparison of all the irreducible representation components of the electrostatic potential shows the same trend, reinforcing the idea that electrostatic effects are sufficiently large to be the principal contributions to the observed experimental splitting.

DISCUSSION

Both optical and IR spectroscopy have been used to evaluate local electric fields in proteins. The effect of electric fields on IR frequency of CO in heme proteins is documented by comparison of proteins with site-directed mutations (*24*), homologous proteins (*21*, *59*), and direct Stark experiments (*31*). Electric fields within the protein are also known to produce heme optical changes (*16*−*18*, *39*). This paper is the first work in which the IR and optical spectra were both examined under the same conditions. Two ways were used to perturb the spectra. The first was to change the pH, which changes the protonation of the distal His. The second was to bind the substrate analogue BHA or NHA to the protein. The orientation and distance of BHA are known from the crystal structure (*6*), thereby allowing for evaluation of its effect on the two chromophores.

To summarize the experimental results, the Q(0,0) absorption band of CO-HRP at pH 6.0 exhibits a single band, but adding substrate or increasing the pH produces a split in the band (Table 1). The fact that the split does not arise from two conformations of the protein seems clear since the IR spectrum of CO shows a single frequency in the absence or presence of the substrate (Figure 5A). The sequence of the split in the bands is ΔQ(low pH) < ΔQ(high pH) < ΔQ(low pH + substrate), the respective values being ∼0, 200, and 320 cm^{-1}. The binding of substrate shifts the CO frequency to higher values, as does increasing the pH (Tables 1 and 2). In this case, the sequence for the frequencies is ν(CO)(low pH) < ν(CO)(low pH + substrate) < ν(CO)(high pH), the respective values being 1903, 1916, and 1936 cm^{-1}. The conclusion of the calculations is that an electrostatic effect can be invoked to explain both the Q(0,0) splitting and the CO stretch frequency shift, including their relative ordering. The ordering of the results can be explained by recognizing that the electrostatic potential is spatially dependent. To illustrate this, the relative positions and orientation of the heme, CO, His42, and BHA are shown in Figure 7. In the case of the CO stretch, the electric dipole can be expected to be approximately coincident with the molecular axis, i.e., along the *z* axis and perpendicular to the heme plane. Therefore, changing the charge along this axis, by deprotonating His42, seen in Figure 7 to be nearly directly above the CO, would have a rather large effect. This result supports our previous theoretical conclusion (*28*, *29*) that the A_{2u} component of the field perpendicular to the porphyrin plane has the major control of ν(CO). In contrast, the Q(0,0) band splitting can be caused only by low-symmetry B_{1g} and B_{2g} components of the electric field, the totally symmetrical components of the field being able only to shift the center of gravity of the Q(0,0) band. In this way, the substrate field has a major influence on the optical spectra, because the electronegative carbonyl region of the substrate BHA is oriented in a manner that would affect the π electron distribution, mainly affecting the B_{1g} component of the electric field. But BHA affects the CO stretch frequency only slightly, since the dipole orientation of CO does not favor an interaction with the field that the substrate produces.

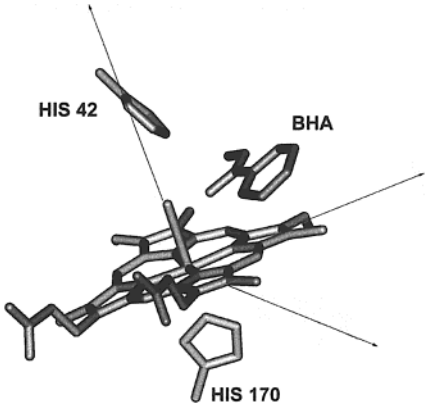

FIGURE 7: Heme of HRP. The distal His, His42, is shown to be bisected by the *z* axis, defined as the axis perpendicular to the heme, with CO lying on this axis. The close distance of the negative carbonyl of BHA to the heme edge can be seen. His170 is also shown.

In the calculation of the electric field, we used the same coordinates for the heme complex for the three experimental conditions, but examined solely the effect of the local field. Our results therefore indicate that the field can account for the spectral changes. This is not to say that there may not be additional influences of the polypeptide chain. We first discuss the effects on the Q(0,0) band. Rasnik et al. have examined various effects on low-spin heme spectra (*18*). It was shown that the spectral splitting of the heme Q(0,0) band is caused by combined contributions from macrocycle conformation, electrostatic field imposed by the protein environment, axial ligation, and the propionic peripheral substituents, and that these effects can be approximately equal in magnitude. Depending on the particular symmetry of each of these perturbations that destroy the ideal D_{4h} symmetry of the heme group, the effects may add or subtract, making the Q(0,0) band splitting highly sensitive to the whole protein structure. The binding of substrate and changing the pH might also be expected to cause changes in the heme pocket and heme conformation that would additionally influence the spectra. It is instructive to compare other low-spin forms of HRP that are formed when porphyrins containing closed shell metals such as Mg or Zn are substituted for the native heme. The Q(0,0) absorption band of the Mg-mesoporphyrin-substituted HRP shows splitting at low temperatures (*13*). The splitting trend is the same as for CO-HRP; that is to say, adding the substrate BHA increases the split in the Q(0,0) band for both MgMP-HRP and CO-HRP (Table 1). In another protein, the absorption spectra of low-spin ferrous cytochromes *c* and the Zn-substituted cytochrome *c* derivatives were compared. Again, the trends in the splittings were conserved upon metal substitution (*16*, *17*). While the Q(0,0) band of low-spin heme complexes is sensitive to symmetry-lowering conditions, whether a split band will be experimentally observed will depend on the bandwidths as well as the splitting value. Since the details of ligation are different for low-spin ferrous and closed shell metal complexes, it suggests that factors involving the ligand per se in these cases are unlikely to be solely causing the split. This would support the argument that other effects such as the local electric field

or the heme conformation contributes to the spectral features. However, this supposition would be strengthened if the structure of the complex were known, allowing for more precise calculation of the spectra. Further comparisons of various ligated forms may help to separate the various effects.

As for the optical spectra, the protein environment affects strongly the CO vibrational frequency in CO-bonded heme protein complexes (*21*, *24*, *26*−*29*, *31*, *60*, *61*). Any condition that changes the electronic density of the CO bond will produce a change in the corresponding stretching frequency (*25*, *27*−*30*). Sterically induced bond distortions, electrostatic fields, hydrogen bonding, and electron back-donation from the heme group can contribute in this way to the observed absorption frequency. The electrostatic contributions to the CO stretching frequencies, as with the perturbative approach of the empirical Stark tuning rate as shown above, gave excellent agreement with the observed experimental shifts. The relatively low frequency of the ν(CO) band in horseradish peroxidase with respect to myoglobin can also be interpreted as a result of the electrostatic environment of the heme. Electrostatic potential differences in C and O atoms for CO-HRP give electrostatic field values of 20, 8, and 16 kcal/mol (or 7.1×10^7, 2.8×10^7, and 5.6×10^7 V/cm) for the conditions of protonated histidine, unprotonated histidine, and substrate binding at neutral pH, respectively.

We should note that the field values for CO in HRP are higher than the ones presented by Phillips et al. for a set of myoglobin proteins (*24*). The higher potential difference is consistent with the lower-frequency range of CO stretch band in horseradish peroxidase, although direct comparison of the systems should be made carefully because of the different environments. Our calculations suggest strongly that electrostatic effects are of major relevance in determining the observed spectral shifts for the CO stretch band, consistent with the conclusion of Phillips and co-workers. In particular, in HRP the electric field of the distal histidine (His42) mainly contributes to (just like in Mb) the pH dependence of the CO frequency. It should be emphasized that with this electrostatic description of the distal histidine we simulate the major contribution to the hydrogen bonding effect, as it is well-known that the hydrogen bonding has a large electrostatic component (*62*, *63*). Indeed, the proximal imidazole ligand forms strong hydrogen bonds with nearby residues over a wide pH interval (*28*). This hydrogen bond can be simulated by locating a unit negative charge located close to the distal nitrogen of the proximal histidine imidazole (*64*). It was shown previously that such a charge must reduce the CO frequency by 20−30 cm^{-1} (*28*). This result is in a very good agreement with the experimental data and strongly supports previous qualitative considerations (*65*).

An analysis of the electrostatic map obtained for the three cases considered in this paper shows that the dipole approximation used in the paper correctly describes the effect of distant charge contributions to the vibrational Stark shift, so the dipole approximation is a good one. Proximal charged species may contribute to the higher multipole moments, as in the case of substrate binding. Because in our work we essentially analyzed three different conditions, we do not have enough points to optimize a choice of the Stark tuning rate (and this is not the purpose of this work). On the basis of their vibrational Stark spectroscopy results, Park et al. suggest that the value used here for the Stark tuning rate is high (*31*). Although their experimental method provides an interesting way of attack, its main source of uncertainty is the evaluation of the actual electric field inside the protein. This limitation is also inherent in our calculation, as we described the protein as a continuum dielectric. The essential conclusions of our work are not affected by a particular choice of the Stark tuning rate. Its exact value is still an open problem, and further study on different systems is essential to reach definite conclusions.

To summarize, shifts of ν(CO) and spectral splitting of the Q(0,0) band of the heme absorption spectrum in CO-HRP occur when the pH is changed and with binding of the substrate. The CO−porphyrin complex provides both optical and IR signals for the study of local environment effects, results that are relevant not only for the particular case studied here but also for all CO-bound heme proteins. We showed that, although limited in accuracy, semiempirical calculations combined with Poisson−Boltzmann electrostatic calculations can give good results when combined with suitably designed experiments. The spectroscopic changes are consistent with the view that they are caused mainly by electrostatic effects. The experimental observation of both electronic and IR spectra, combined with the various methods of spectral calculation, shows new possibilities for characterization of the pocket in heme proteins, since by the directionality of the interactions, they probe different parts of the protein. The spectroscopic changes in the heme proteins can be studied in solution over a wide range of temperature and experimental conditions so they can also provide important information about dynamical effects. The quantitative description of the environment and its effects on the heme electronic structure, reflected in its optical spectra, provide an important step to understanding the modulation of activity by the protein environment.

ACKNOWLEDGMENT

We thank Dr. Kim Sharp for helpful discussions and the use of computers and computer programs.

REFERENCES

1. Chance, B. (1949) *Science 109*, 204−208.
2. Schejter, A., Lanir, A., and Epstein, N. (1976) *Arch. Biochem. Biophys. 174*, 36−44.
3. Schonbaum, S. R. (1973) *J. Biol. Chem. 248*, 502−511.
4. Paul, K.-G., and Ohlsson, P.-I. (1978) *Acta Chem. Scand., Ser. B 32*, 395−404.
5. Gajhede, M., Schuller, D. J., Henriksen, A., Smith, A. T., and Poulos, T. L. (1997) *Nat. Struct. Biol. 4*, 1032−1038.
6. Henriksen, A., Schuller, D. J., Meno, K., Welinder, K. G., Smith, A. T., and Gajhede, M. (1998) *Biochemistry 37*, 8054−8069.
7. Henriksen, A., Smith, A. T., and Gajhede, M. (1999) *J. Biol. Chem. 274*, 35005−35011.
8. Leigh, J. S., Maltempo, M. M., Ohlsson, P. I., and Paul, K. G. (1975) *FEBS Lett. 51*, 304−308.
9. Sakurada, J., Takahashi, S., and Hosoya, T. (1986) *J. Biol. Chem. 261*, 9657−9662.
10. Chang, Y.-T., Veitch, N. C., and Loew, G. H. (1998) *J. Am. Chem. Soc. 120*, 5168−5178.
11. Kertez, D., Antonini, E., Brunori, M., Wyman, J., and Zito, R. (1965) *Biochemistry 4*, 2672−2676.
12. Gouterman, M. (1961) *J. Mol. Spectrosc. 6*, 138−163.
13. Balog, E., Kis-Petik, K., Fidy, J., Kohler, M., and Friedrich, J. (1997) *Biophys. J. 73*, 397−405.

14. Suisalu, A., Mauring, K., Kikas, J., Herenyi, L., and Fidy, J. (2001) *Biophys. J. 80*, 498−504.
15. Reddy, K. S., Angiolillo, P. J., Wright, W. W., Laberge, M., and Vanderkooi, J. M. (1996) *Biochemistry 35*, 12820−12830.
16. Manas, E., Vanderkooi, J. M., and Sharp, K. (1999) *J. Phys. Chem. B 103*, 6334−6348.
17. Manas, E. S., Wright, W. W., Sharp, K. A., Friedrich, J., and Vanderkooi, J. M. (2000) *J. Phys. Chem. B 104*, 6932−6941.
18. Rasnik, I., Sharp, K., Fee, J. A., and Vanderkooi, J. M. (2001) *J. Phys. Chem. B 105*, 282−286.
19. Springer, B. S., Sligar, S. G., Olson, J. S., and Phillips, G. N., Jr. (1994) *Chem. Rev. 94*, 699−714.
20. Li, T., Quillin, M. L., Phillips, G. N., Jr., and Olson, J. S. (1994) *Biochemistry 33*, 1433−1446.
21. Laberge, M., Vanderkooi, J. M., and Sharp, K. A. (1996) *J. Phys. Chem. 100*, 10793−10801.
22. Karavitis, M., Fronticelli, C., Brinigar, W. S., Vasquez, G. B., Mititello, V., Leone, M., and Cupane, A. (1998) *J. Biol. Chem. 273*, 23740−23749.
23. Feis, A., Rodriguez-Lopez, J. N., Thorneley, R. N. F., and Smulevich, G. (1998) *Biochemistry 37*, 15575−15581.
24. Phillips, G. N., Jr., Teodoro, M. L., Li, T., Smith, B., and Olson, J. S. (1999) *J. Phys. Chem. B. 103*, 8817−8829.
25. Hu, S., Vogel, K. M., and Spiro, T. G. (1994) *J. Am. Chem. Soc. 116*, 11187−11188.
26. Laberge, M., Sharp, K. A., and Vanderkooi, J. M. (1997) *J. Phys. Chem. 101*, 7364−7367.
27. Kushkuley, B., and Stavrov, S. S. (1997) *Biochim. Biophys. Acta 1341*, 238−250.
28. Kushkuley, B., and Stavrov, S. S. (1997) *Biophys. J. 72*, 899−912.
29. Kushkuley, B., and Stavrov, S. S. (1996) *Biophys. J. 70*, 1214−1229.
30. Vogel, K. M., Kozlowski, P. M., Zgierski, M. Z., and Spiro, T. G. (1999) *J. Am. Chem. Soc. 121*, 9915−9921.
31. Park, E. S., Andrews, S. S., Hu, R. B., and Boxer, S. G. (1999) *J. Phys. Chem. B 103*, 9813−9817.
32. Kaposi, A. D., Fidy, J., Manas, E. S., Vanderkooi, J. M., and Wright, W. W. (1999) *Biochim. Biophys. Acta 1435*, 41−50.
33. Paul, K.-G. (1958) *Acta Chem. Scand. 12*, 1312−1318.
34. Wright, W. W., Laberge, M., and Vanderkooi, J. M. (1997) *Biochemistry 36*, 14724−14732.
35. Nicholls, A., and Honig, B. (1991) *J. Comput. Chem. 12*, 435−445.
36. Jayaram, B., Sharp, K. A., and Honig, B. (1989) *Biopolymers 28*, 975−993.
37. Gilson, M. K., Sharp, K. A., and Honig, B. (1987) *J. Comput. Chem. 9*, 327−335.
38. Sharp, K., and Honig, B. (1990) *Annu. Rev. Biophys. Chem. 19*, 301−332.
39. Anni, H., Vanderkooi, J. M., Sharp, K. A., Yonetani, T., Hopkins, S. C., Herenyi, L., and Fidy, J. (1994) *Biochemistry 33*, 3475−3486.
40. Frisch, M. J., Trucks, G. W., Schlegel, H. B., Gill, P. M. W., Johnson, B. G., Robb, M. A., Cheeseman, J. R., Keith, T., Petersson, G. A., Montgomery, J. A., Raghavachari, K., Al-Laham, M. A., Zakrzewski, V. G., Ortiz, J. V., Foresman, J. B., Cioslowski, J., Stefanov, B. B., Nanayakkara, A., Challacombe, M., Peng, C. Y., Ayala, P. Y., Chen, W., Wong, M. W., Andres, J. L., Repogle, E. S., Gomperts, R., Martin, R. L., Fox, D. J., Binkley, J. S., Defrees, D. J., Baker, J., Stewart, J. P., Head-Gordon, M., Gonzalez, C., and Pople, J. A. (1995) *Gaussian 94, Revision E.2*, Gaussian, Pittsburgh, PA.
41. Lambert, D. K. (1988) *J. Chem. Phys. 89*, 3847−3860.
42. Bacon, A. D., and Zerner, M. C. (1979) *Theor. Chim. Acta 53*, 21−54.
43. Ridley, J., and Zerner, M. C. (1973) *Theor. Chim. Acta 32*, 111−134.
44. Ridley, J. E., and Zerner, M. C. (1976) *Theor. Chim. Acta 42*, 223−236.
45. Ma, J.-G., Laberge, M., Song, Z.-Z., Jentzen, W., Jia, S.-L., Vanderkooi, J. M., and Shelnutt, J. A. (1998) *Biochemistry 37*, 5118−5128.
46. Jentzen, W., Ma, J.-G., and Shelnutt, J. A. (1998) *Biophys. J. 74*, 753−763.
47. Jentzen, W., Simpson, M. C., Hobbs, J. D., Song, X., Ema, T., Nelson, N. Y., Medforth, C. J., Smith, K. M., Veyrat, M., Mazzanti, M., Ramasseul, R., Marchon, J.-C., Takeuchi, T., Goddard, W. A. I., and Shelnutt, J. A. (1995) *J. Am. Chem. Soc. 117*, 11085−11097.
48. Tinkham, M. (1964) *Group Theory and Quantum Mechanics*, McGraw-Hill, New York.
49. Gouterman, M. (1959) *J. Chem. Phys. 30*, 1139−1161.
50. Gouterman, M. (1978) in *The Porphyrins* (Dolphin, D., Ed.) pp 1−156, Academic Press, New York.
51. Tamura, M., Asakura, T., and Yonetani, T. (1972) *Biochim. Biophys. Acta 268*, 292−304.
52. Uno, T., Nishimura, Y., Tsuboi, M., Makino, R., Iizuka, T., and Ishimura, Y. (1987) *J. Biol. Chem. 262*, 4549−4556.
53. Teraoka, J., and Kitagawa, T. (1981) *J. Biol. Chem. 256*, 3969−3977.
54. Meunier, B., Rodriguez-Lopez, J. N., Smith, A. T., Thorneley, R. N., and Rich, P. R. (1998) *Biochem. J. 330*, 303−309.
55. Balog, E., Galantai, R., Kohler, M., Laberge, M., and Fidy, J. (2000) *Eur. Biophys. J. 29*, 429−438.
56. Smulevich, G., Evangelista-Kirkup, R., English, A., and Spiro, T. G. (1986) *Biochemistry 25*, 4426−4430.
57. Barlow, C. H., Ohlsson, P.-I., and Paul, K.-G. (1976) *Biochemistry 15*, 2225−2229.
58. Holzbaur, I. E., English, A. M., and Ismail, A. A. (1996) *J. Am. Chem. Soc. 118*, 3354−3359.
59. Laberge, M., Sharp, K. A., and Vanderkooi, J. M. (1998) *Biophys. Chem. 71*, 9−20.
60. Ray, G. B., Li, X.-Y., Ibers, J. A., Sessler, J. L., and Spiro, T. G. (1994) *J. Am. Chem. Soc. 116*, 162−176.
61. Park, K. D., Guo, K., Adebodun, F., Chiu, M. L., Sligar, S. G., and Oldfield, E. (1991) *Biochemistry 30*, 2333−2347.
62. Jeffrey, G. A. (1997) *An Introduction to Hydrogen Bonding*, Oxford University Press, New York.
63. Umeyama, H., and Morokuma, K. (1977) *J. Am. Chem. Soc. 99*, 1316−1333.
64. Finzel, B. C., Poulos, T. L., and Kraut, J. (1984) *J. Biol. Chem. 259*, 13027−13036.
65. Evangelista-Kirkup, R., Smulevich, G., and Spiro, T. G. (1986) *Biochemistry 25*, 4420−4425.

BI002784Z